# Isolation and Characterization of a Novel *n*-Alkane-Degrading Strain, *Acinetobacter haemolyticus* AR-46

Zoltán Bihari[a,*], Aladár Pettkó-Szandtner[b], Gyula Csanádi[c], Margit Balázs[a], Péter Bartos[a], Péter Kesserű[a], István Kiss[a], and Imre Mécs[a]

[a] Institute for Biotechnology, Bay Zoltán Foundation for Applied Research, Derkovits fasor 2., H-6726 Szeged, Hungary. E-mail: bihari@bay.u-szeged.hu
[b] Institute of Plant Biology, Biological Research Centre, Hungarian Academy of Sciences, Temesvári körút 62., P. O. Box 521, H-6701 Szeged, Hungary
[c] Department of Biotechnology, University of Szeged, Temesvári körút 62., H-6701 Szeged, Hungary

* Author for correspondence and reprint requests

Z. Naturforsch. **62c**, 285–295 (2007); received November 14/December 6, 2006

Strain AR-46, isolated and identified as *Acinetobacter haemolyticus*, evolutionally distant from the known hydrocarbon-degrading *Acinetobacter* spp., proved to have excellent long-chain *n*-alkane-degrading ability. This is the first detailed report on an *n*-alkane-utilizing strain belonging to this species. The preferred substrate is *n*-hexadecane, with an optimal temperature of 37 °C under aerobic conditions. Five complete and two partial open reading frames were sequenced and correlated with the early steps of monoterminal oxidation-initiated *n*-alkane mineralization. The encoded protein sequences and the arrangement of these genes displayed high similarity to those found in *Acinetobacter* sp. M-1, but AR-46 seemed to have only one alkane hydroxylase gene, with a completely different induction profile. Unique behaviour was also observed in *n*-alkane bioavailability. Substrate uptake occurred through the hydrophobic surface of *n*-alkane droplet-adhered cells possessing long, thick fimbriae, which were presumed to play a major role in *n*-alkane solubilization. A majority of the cells was in detached form, with thick, but short fimbriae. These free cells were permanently hydrophilic, unlike the cells of other *Acinetobacter* strains.

*Key words:* *n*-Alkane, *alkM* Induction, Direct Adherence

## Introduction

Various Gram-positive and Gram-negative bacteria are applied on an industrial scale as oil degraders (Radwan *et al.*, 1995; Ward *et al.*, 2003), but exclusively members of the *Acinetobacter* genus are capable of depleting the very long-chain *n*-alkane fraction of crude oil. In general, *Acinetobacter* spp. can utilize *n*-alkanes as the sole source of carbon and energy, if they have carbon chain lengths of from $C_6$ (Huy *et al.*, 1999) up to $C_{44}$ (Sakai *et al.*, 1994), via monoterminal oxidation (Koma *et al.*, 2001) or the Finnerty pathway (Maeng *et al.*, 1996). *n*-Hexadecane is frequently used as a model substrate to investigate the *n*-alkane-degrading ability, but limited information is available (Hori *et al.*, 2002) on the kinetic parameters of microbial growth during the biodegradation of *n*-alkanes, and the temperature dependence of *n*-alkane mineralization by the relevant *Acinetobacter* spp. has not been reported at all.

To achieve a sufficient hydrocarbon biodegradation rate, a number of different uptake mechanisms have been evolved in the *Acinetobacter* genus. *A. venetianus* RAG-1 secretes emulsan, a heteropolysaccharide bioemulsifier (Goldman *et al.*, 1982), and releases alkane-solubilizing membrane-bound vesicles (Sullivan *et al.*, 1999). Besides bioemulsification, the bioavailability is enhanced by specific cell adherence to the alkane substrate. Rosenberg *et al.* (1982) presumed that thin (ca. 3.5 nm diameter) fimbriae are responsible for this process, but emulsan-deficient, thin fimbriae-deficient mutants of RAG-1 proved to have the same growing capacity as that of the wild strain (Pines and Gutnick, 1984). These results indicate the crucial role of still unidentified hydrophobic membrane sites or cell components in direct adherence. The microbial adhesion to hydrocarbon (MATH) test has demonstrated that the surface of RAG-1 cells is permanently hydrophobic, irrespectively of the nature of the added carbon source. Bioemulsifier production has not been observed in *A. venetianus* VE-C3; the cells are originally hydrophilic, but become hydrophobic after exposure to *n*-alkanes (Baldi *et al.*, 1999).

0939–5075/2007/0300–0285 $ 06.00 

Once the substrate becomes bioavailable and penetrates the cell membrane, multi-step oxidation processes occur. In the case of the well-characterized and complete genome-sequenced *A.* sp. ADP1, the first step of *n*-alkane oxidation is catalyzed by a non-heme iron integral membrane alkane hydroxylase/monooxygenase (1.14.15.3). This protein, responsible for monoterminal alkane degradation, is encoded by the *alkM* gene (Ratajczak *et al.*, 1998a). Its expression, induced by a broad range of *n*-alkanes ($C_7$–$C_{18}$), requires the transcriptional activator AlkR, an AraC-XylS-like protein expressed at a low level. The transcription of the complement *alkR* gene is indispensable for *n*-alkane degradation, but the growth-supporting substrate range mainly depends on the induction of *alkM*. Weakly conserved putative promoter elements and an inverted repeat target site for the regulator protein have been identified upstream from *alkM* (Ratajczak *et al.*, 1998b). Two *alkM* and *alkR* paralogues representing different regulation mechanisms have been found in *A.* sp. M-1 (Tani *et al.*, 2001). The *alkMa* gene is induced by solid *n*-alkanes with chain lengths longer than $C_{22}$, while *alkMb* expression is evoked by $C_{16}$–$C_{22}$ *n*-alkanes. In the upstream regions of *alkMa* and *alkMb*, the *alkRa* and *alkRb* genes are located in complement orientations coding for AraC-XylS-like and OruR-like regulator proteins, respectively.

Despite the importance of the alkane-degrading microbes in this genus, only few strains have been characterized in detail in connection with their biodegradation rates, uptake processes and gene regulations. The present paper reports these properties for a novel *Acinetobacter* strain with special *n*-alkane oxidation and uptake features.

## Materials and Methods

### *Taxonomic characterization of the bacterium*

16S rDNA analysis was performed directly on an AR-46 colony resuspended in 1 M glycine-betaine buffer, using the PCR method described by Di Cello *et al.* (1997). The 1413 bp partial nucleotide sequence of the 16S rDNA gene has been submitted to the GenBank database and is reported under accession number AY586400.

The biochemical characterization of isolate AR-46 was carried out in accordance with Vaneechoutte *et al.* (1999). After identification, the isolated bacterium was deposited in the Hungarian National Collection of Agricultural and Industrial Microorganisms under accession number NCAIM B02172.

### *Cultivation conditions*

Cells were routinely cultivated in 100-ml Erlenmeyer flasks containing 50 ml of high-nitrogen-phosphorus-sulfur (HNPS) (Leahy *et al.*, 2003) or low-nitrogen-phosphorus-sulfur (LNPS) (Snellman *et al.*, 2002) medium supplemented with 1 g/l of *n*-hexadecane. For determination of the utilizable hydrocarbon spectrum, 1 g/l of different *n*-alkanes (with a chain length from $C_6$ to $C_{40}$) or aromatic hydrocarbons was added as carbon source. Media were inoculated with 0.5 ml of the 24-h culture grown on DSM1 complete medium. Before inoculation, cells were centrifuged ($16{,}000 \times g$, 5 min) and resuspended in the inorganic medium. Flasks were incubated for appropriate, regular time intervals under non-stirred conditions at 37 °C, or at 25–40 °C in the temperature dependence experiments. Microbial growth was followed via the increases in optical density (OD) and cell dry weight of the cultures. Total cell numbers were counted microscopically too. Fermentation kinetic parameters were calculated according to the Monod model.

### *Analytical procedures*

*n*-Hexadecane degradation by strain AR-46 was analyzed by gas chromatography (GC) after chloroform/methanol (3:1) extraction (Koma *et al.*, 2001). 2 $\mu$l of the organic phase were injected into a HP-5890 Series II GC instrument fitted with a HT-5 capillary column (SGE 25 m × 0.32 mm × 0.1 $\mu$m) and an FID detector. The analysis conditions were as follows: injector and detector temperature, 280 °C; column temperature, 100 °C for 1 min, then increased to 250 °C at a rate of 15 °C/min in split mode (1:20).

For identification of intermediates of the *n*-hexadecane biodegradation pathway, the strain was cultivated in 500 ml of HNPS or LNPS medium supplemented with 1 g/l of carbon source. Cells were harvested in midlog and early stationary phases and washed twice with physiological saline solution. The resuspended cells were sonicated on ice for 1.5 min 3 times at 25 W (Vibracell, Sonics & Materials, USA). The total crude extract was applied directly for enzyme assays or was further extracted with an equal volume of chloroform/methanol (4:1) for intermediate analysis. 2 $\mu$l of the

concentrated chloroform layer were analyzed directly (without methanolysis) on a Finnigan ThermoQuest Trace GC/Automass GC-MS instrument fitted with a DB-5 capillary column (30 m × 0.25 mm × 0.25 $\mu$m) in splitless mode. The conditions of analysis were as follows: injector and detector temperature, 350 °C; column temperature, 45 °C for 1 min, then increased to 330 °C at a rate of 15 °C/min and held at 330 °C for 15 min.

MATH tests (Baldi *et al.*, 1999) and OD measurements were made with a Unicam Helios $\alpha$ spectrophotometer at 600 nm. Surface tension measurements (Traube procedure) (Vold and Vold, 1983), GC *n*-hexadecane partition analysis (Käppeli and Finnerty, 1979), emulsification assays (Rosenberg *et al.*, 1979), and total carbohydrate (Dubois *et al.*, 1951) and protein (Bradford, 1976) measurements were carried out as described previously. Alkane dioxygenase (Sakai *et al.*, 1996) and cytochrome P-450 activities (Müller *et al.*, 1989) of enzyme preparations were also determined. All measurements were performed in triplicate.

### *Microscopic study of A. haemolyticus AR-46*

For transmission electron microscopy (TEM), non-adhered cells were sampled from the bulk phase of the culture by submerging the pipette carefully below the level of the *n*-hexadecane-adhered cell layer. The whole culture was then centrifuged (16,000 × *g*, 10 min) and the adhered cells were sampled from the surface layer containing *n*-alkane-attached cells. Finally, both cell types were treated as described previously (Rosenberg *et al.*, 1982). Grids were examined with a Tecnai-12 (FEI) electron microscope. Photos were taken with a CCD camera (MegaView III, Soft Imaging System). For light microscopy, cells were observed with a Zeiss Axiskop 20 microscope.

### *DNA manipulations*

Genomic (Wilson, 1994) and plasmid (Engebrecht *et al.*, 1991) DNA was isolated according to standard protocols. For the amplification of *alkM* gene(s), degenerated primers (AlkDegFw and AlkDegRev; see Table I) were designed on the basis of the conserved regions between the *alkB* and *alkM* sequences of 10 *n*-alkane-degrading *Pseudomonas* and *Acinetobacter* strains. Touchdown PCR was performed in 50 $\mu$l of Promega buffer supplemented with 1.25 mM $MgCl_2$, 250 $\mu$M of each dNTP, 2 U of Taq, 0.5 $\mu$M of each primer and 100 ng of the genomic template DNA of strain AR-46. The PCR program was 11 × [0.5 min at 95 °C, 0.5 min at 68 − i °C (i = 1 − 11]) and 1 min at 72 °C], and then 20 × (0.5 min at 95 °C, 0.5 min at 55 °C, and 1 min at 72 °C). The reaction yielded an *alkM* fragment. Inner AlkInv1Fw and AlkInv1-Rev primers were designed on the basis of the sequence of this product, and used in inverse PCR. The *Eco*RI-digested chromosomal DNA of strain AR-46 was self-ligated and applied as a template. The touchdown PCR protocol described above was set up with 6-min elongation periods. The amplified fragment was sequenced through consecutively by the newly designed inverse primers (Table I). Finally, the entire sequence of the *Eco*RI-ended part of genomic DNA was assembled; it is reported under accession number AY586401 in the GenBank.

Table I. Sequences of primers used in this study.

| Primer | Sequence (5′→3′) |
|---|---|
| AlkDegFw: | TTCCNRYGATHGATACRATTATTGG |
| AlkDegRev: | CGHGTCGGATWVGCGTGATGATC |
| AlkInv1Fw: | GGTTGGGGCATGAGTGCTGCATTTC |
| AlkInv1Rev: | GATCGCCCCCATTGAAACACCAAGC |
| AlkInv2Fw: | GCTCATCATGTTCCAAGCACTG |
| AlkInv2Rev: | CATCGTCGTATCCATGTCTTCG |
| AlkInv3Fw: | CGATTGCCTCTGACGCTCAG |
| AlkInv3Rev: | CAGCGCCTGAATGGCTGC |
| AlkInv4Rev: | GCAGTTCTTAGCCCCTGAATCG |
| AlkInv5Rev: | CAAGCTGGTCACCCGCAACAAC |

For the determination of amino acid and DNA sequence similarities, the ClustalW program of EBI was used. Bacterial promoter prediction was performed with the BPROM software of SoftBerry. The topology of proteins and transmembrane helices was predicted with the HMMTOP software of the Hungarian Academy of Sciences.

### *Southern and Northern blot analyses*

Southern blot analysis was carried out by using the *alkM* fragment as the probe on the genomic DNA digested with various restriction enzymes (*Xho*I, *Hin*dIII and *Eco*RI). The hybridization was performed under high-stringency (66 °C) and low-stringency (37 °C) conditions, using the Gene Images Random Prime Labelling module and the Gene Images CDP-Star Detection module (Amersham Life Science) in accordance with the manufacturer's instructions.

The effects of different *n*-alkane carbon sources on the expression of the *alkM* gene were determined by Northern blot analyses. AR-46 cells were cultivated on control rich media (DSM1) and on *n*-dodecane, *n*-hexadecane, *n*-eicosane and *n*-triacontane under the conditions described above. Total RNA extracted from midlog phase cells was isolated by using the Trizol reagent (Amersham Pharmacia Biotech, Little Chalfont, UK). 20 $\mu$g of total RNA were run on 1% formaldehyde gel containing 0.01% ethidium bromide. RNAs were transferred to Amersham Hybond N filters through the classical upward technique, and the ribosomal RNA patterns of the filters were examined under UV light in order to verify the efficiency of transfer and the quality of the loaded RNA. Radioactive labelling and hybridization were carried out by the standard protocols supplied by Amersham. The filter was exposed to a phosphor storage screen for 12 h, and analyzed with a Molecular Dynamics 860 STORM PhosphorImager. The signal intensities of the ribosomal RNA and the radioactively labelled *alkM* RNA were quantified with ImageQuant 5.0 software (Molecular Dynamics, Sunnyvale, California, USA).

## Results

### *Isolation and classification of strain AR-46*

In order to isolate hydrocarbon-degrading bacteria, Hungarian oil wells were screened: HNPS minimal medium supplemented with 1 g/l of purified, solid paraffins ($C_{20}-C_{38}$ fraction) as sole carbon source was inoculated with production water from the wells and incubated at 30 or 37 °C under static conditions. Fractions of cultures exhibiting microbial growth were used for reinoculation several times and finally purified for single colonies. The dominant isolate (AR-46) grown at 37 °C was used for further studies. For initial classification, a segment of its 16S rDNA was amplified and the product was sequenced. The 1413 bp sequence displayed the highest similarity (99.86% and 99.51% identity) to the ammonia oxidizer *Acinetobacter* sp. YY-5 (AY639376) and the type strain *A. haemolyticus* DMS 6962$^T$ (X81662), respectively. Comparison with the available *Acinetobacter* 16S

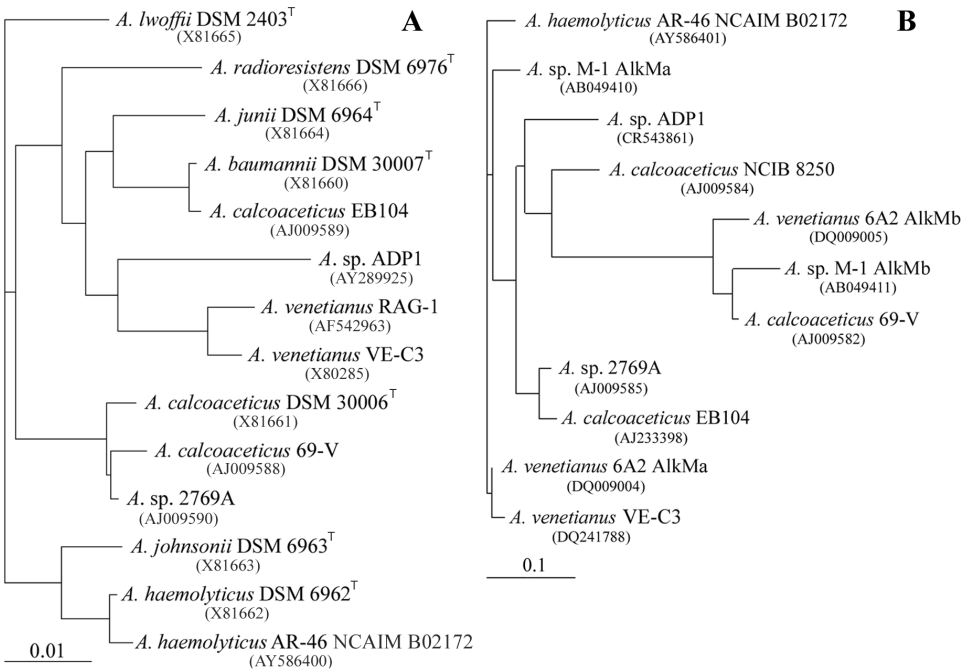


Fig. 1. Unrooted phylogenetic trees based on aligned *Acinetobacter* 16S rDNA (A) and alkane hydroxylases (B) sequences generated by the ClustalW program. The GenBank accession numbers of relevant oil-degrading isolates and type strains (with DSM accession numbers and $^T$ symbols) are given in parenthesis. The bars denote 1 nucleotide substitution per 100 nucleotides (A) and 10 substitutions per 100 amino acids (B).

rDNA sequences revealed that the isolate was evolutionally distant from the known hydrocarbon-degrading *Acinetobacter* isolates, but very similar to the type strain *A. haemolyticus* DSM 6962$^T$ (Fig. 1A).

To confirm that this Gram-negative coccus really is a member of the *A. haemolyticus* species, further biochemical characterization was performed: The strain was beta-haemolytic, produced beta-xylosidase, created acid from glucose, and demonstrated growth at 41 °C and on 4-hydroxybenzoate, but not on lactate or malonate. In view of these determinative biochemical properties and the similarity of the 16S rDNA sequences, we concluded that isolate AR-46 is indeed a member of the *A. haemolyticus* species.

### *Determination of the hydrocarbon-degrading ability*

The substrate specificity of the isolate was investigated by using different *n*-alkanes as carbon source at 37 °C (Fig. 2). Strain AR-46 catabolized liquid *n*-alkanes to a greater extent than solid ones, and *n*-hexadecane was found to be the best of the examined substrates for growth. GC measurements demonstrated that this bacterium was able to deplete solid paraffins; *n*-$C_{35}$ was the largest compound that underwent a significant decrease in concentration during the 7-day incubation period (data not shown). Hydrophobic aromatic compounds such as toluene, xylene, naphthalene and benz[a]anthracene were not consumed by this microbe.

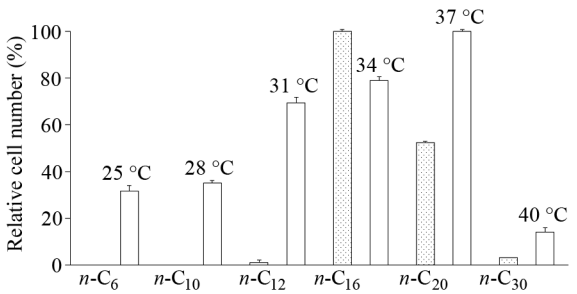


Fig. 2. Substrate and temperature dependences of *n*-alkane utilization of *A. haemolyticus* AR-46. Cells were grown for 48 h on HNPS broth supplemented with 1 g/l of different *n*-alkanes (dotted columns) or with 1 g/l of *n*-hexadecane at 25–40 °C (open columns) under non-stirred conditions. The starting cell number was $5 \times 10^6$ cells/ml. The presented values are total cell number percentages relative to the maximum cell numbers (approximately $7.7 \times 10^8$ cells/ml) attained on the *n*-$C_{16}$ carbon source at 37 °C.

The optimal temperature of *n*-hexadecane mineralization by AR-46 was found to be 37 °C (Fig. 2), while the maximum specific growth rate of the cells ($\mu_m$) was 0.253 $h^{-1}$ and the yield factor for the cells ($Y'_{X/S}$) was 0.576 kg of cells (kg of *n*-hexadecane)$^{-1}$. The hydrocarbon utilization at 37 °C was found not to be a unique phenomenon among related *Acinetobacter* strains. *A. venetianus* 6A2 and *A. calcoaceticus* EB104 were likewise able to grow better on *n*-hexadecane at 37 °C than at 30 °C. However, while strain 6A2 grew similarly to AR-46, the total number of cells achieved by strain EB104 was only (24.3 ± 0.7)% of that achieved by AR-46. The lower temperature, *i. e.* 30 °C, was preferred by *A.* sp. ADP1, *A.* sp. 2769A, *A. calcoaceticus* NCIB 8250 and *A. calcoaceticus* 69-V, but corresponding cell numbers achieved were only (27.0 ± 1.9), (11.7 ± 0.6), (13.3 ± 0.1) and (32.8 ± 0.1)%, respectively, relative to AR-46 at 37 °C. Moreover, even the highest of these latter values is less than half that achieved by AR-46 at 30 °C.

### *The n-alkane uptake mechanism of A. haemolyticus AR-46*

The high *n*-hexadecane biodegradation rate indicated the existence of an efficient uptake mechanism in isolate AR-46. During growth on *n*-hexadecane, the surface tension of the medium did not decrease, and no emulsification activity, or carbohydrate and protein biopolymers were observed in the centrifuged supernatant. *n*-Hexadecane partition analysis revealed that no supernatant from any period of growth elevated the *n*-hexadecane concentration above the corresponding solubility, *i. e.* the AR-46 cells did not secrete biosurfactants, bioemulsifiers or membrane-bound vesicles into the media, indicating that the *n*-alkane uptake occurs by direct cell adherence to the substrate.

Under aerobic, non-stirred conditions, some of the cells did in fact adhere to the surface of the *n*-alkane droplets and made them visible as a semi-transparent cortex (Fig. 3A). This interaction was strong enough to be maintained during intensive centrifugation (16,000 × *g*, 10 min). The TEM picture of the *n*-hexadecane-adhered cells (Fig. 3B) revealed that these cells have only very long (700–1400 nm), thick (11–14 nm) fimbriae. The morphology of the non-adhered cells (Fig. 3C) was

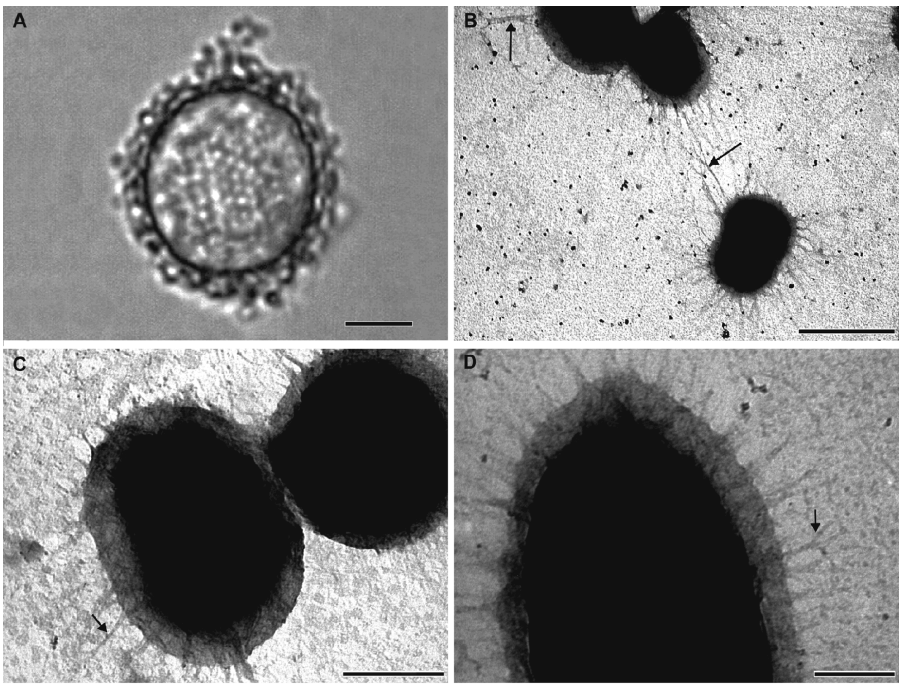


Fig. 3. Micrographs of *A. haemolyticus* AR-46 cells in the late exponential phase of growth. (A) Light microscopy of cell adherence to the surface of an *n*-hexadecane droplet (13 $\mu$m in diameter). In consequence of the three-dimensional adherence to the droplet, the light microscopic picture can not show sharp cell forms. TEM of adhered (B), non-adhered (C) and control cells (D) maintained in complete medium. Longer arrows indicate long fimbriae of adhered cells, while smaller arrows denote normal fimbriae. Scale bars: (A) 5 $\mu$m; (B) 1 $\mu$m; (C) 0.5 $\mu$m; (D) 0.2 $\mu$m.

similar to that of the cells maintained in complete broth (DSM1) (Fig. 3D), but their fimbriae proved significantly shorter (370–440 nm), though the thickness was about the same.

These morphological phenomena correlated well with the cell hydrophobicity values measured in the MATH test. The surface of the non-adhered, free *A. haemolyticus* AR-46 cells remained hydrophilic after exposure to *n*-hexadecane. The measured value of $\log(A_t/A_0 \times 100)$ was higher than 1.95 at every point of the growth curve. This means that fewer than 10% of the free cells were able to adhere to the added *n*-hexadecane substrate. A similar constant surface hydrophilicity was observed when AR-46 was grown on DSM1, glucose or 4-hydroxybenzoate.

### *Determination of pathway of n-hexadecane catabolism in strain AR-46*

From *n*-hexadecane-grown *A. haemolyticus* AR-46 cells, the GC-MS analysis identified *n*-hexadecan-1-ol and *n*-hexadecan-1-oic acid as intermediates of the monoterminal oxidation pathway from the beginning of the log phase, regardless of the medium (HNPS or LNPS) used (mass spectra not shown). The wax ester storage material *n*-hexadecyl-*n*-hexadecanoate was also detected accumulated in cells cultivated in both types of media in the late log phase of growth.

Finnerty pathway-specific alkane dioxygenase activity was not detected in either the soluble or the particulate enzyme fraction of AR-46 cells, irrespectively of the growth phase of the harvested cells. The enzyme activity could not be restored by adding reduced NAD, NADP or FAD as cofactors. Similarly, no significant cytochrome P-450 activity was measured in any enzyme preparation.

These results strengthened the presumption of the involvement of an *alkM* encoded non-heme iron integral membrane alkane hydroxylase, the first key enzyme in the monoterminal oxidation pathway. To prove the role of *alkM* in *n*-alkane degradation by strain AR-46, its PCR-based identification was performed first.

*Identification and analysis of genes that can take part in early steps of n-alkane hydroxylation*

A comparison of the *alkB* and *alkM* protein sequences revealed evolutionally conserved regions. A pair of degenerated oligonucleotides designed for these regions was used in PCR. Although the *alkB* genes are encoded on plasmids in *Pseudomonas* spp., genomic DNA was applied in the further experiments, because we could not detect any plasmid in AR-46. The PCR yielded a 720 bp fragment from the AR-46 genomic DNA template. This product was sequenced and found to be part of an *alkM* gene. This sequence was used as starting point for a description of the full *alkM* and adjacent genes by inverse PCR. On use of the inner AlkInv1Fw and AlkInv1Rev inverse primers, the reaction yielded a 5136 bp fragment. After the sequencing of the inverse PCR product, a 5445 bp long, *Eco*RI-ended sequence was assembled containing 5 complete and 2 partial ORFs.

The gene mapped to ORF6 was *alkM* in strain AR-46. The deduced amino acid sequence and hydrophobicity analysis revealed the typical conserved 8-histidine motif and 5 transmembrane helices (data not shown). The encoded AlkM protein (412 aa) exhibited the greatest similarity to the *alkMa*-encoded partial alkane hydroxylase A sequence of *A. venetianus* 6A2 (96%), to the partial AlkM of *A. venetianus* VE-C3 (94%) and to the complete alkane hydroxylase A sequence of *A.* sp. M-1 (93%). The phylogenetic tree of known alkane hydroxylases is presented in Fig. 1B.

In order to investigate the harbouring of a possible *alkM* gene counterpart, Southern hybridization experiments were performed. Even under low-stringency conditions (37 °C), the labelled 720 bp probe hybridized to one band of genomic DNA digested with different restriction enzymes (Fig. 4A). The sizes of the hybridized *Hin*dIII and *Eco*RI-digested fragments correlated perfectly with their sequence-based expected lengths.

In Northern hybridization analysis, the 720 bp probe hybridized strongly to one band of expressed RNA prepared from cells maintained on *n*-hexadecane, *n*-eicosane or *n*-triacontane, but there was no significant sign of hybridization to RNA from cells grown on *n*-dodecane and DSM1 complete medium (Figs. 4B, D).

The *alkM* of strain AR-46 is induced by different long-chain *n*-alkanes via a putative promoter. This seems to be confirmed by BPROM software-based bacterial promoter prediction and sequence

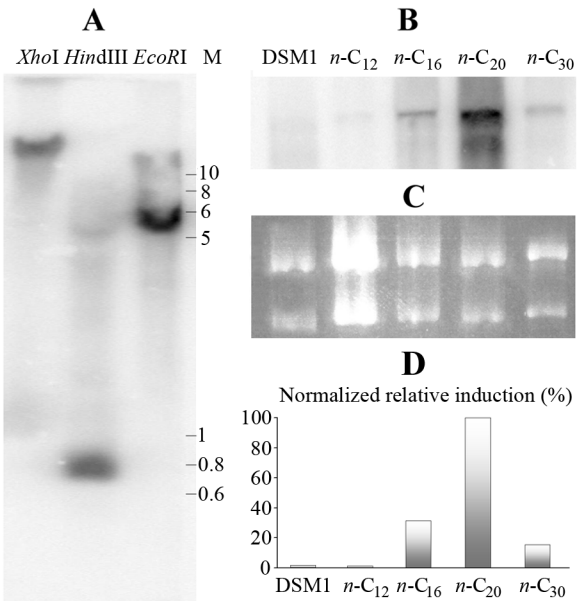


Fig. 4. (A) Southern blot analysis of genomic DNA of *A. haemolyticus* AR-46 digested with various restriction enzymes, its fluorescein-labelled 720 bp *alkM* fragment being used as a probe. Lane M: SmartLadder marker (kbps). (B) Northern blot analysis of expressed RNAs purified from AR-46 cells maintained on different carbon sources. (C) Gel picture of ribosomal RNA controls. (D) Normalized relative induction of the *alkM* gene by *n*-alkanes. Values denote 16S RNA-normalized *alkM* RNA quantities relative to the RNA expressed due to *n*-$C_{20}$.

similarity comparisons, which revealed a putative ribosome binding site, a transcription initiation site, and −10 and −35 boxes located 7, 34, 42 and 62 bp upstream, respectively, from the ATG start codon of the *alkM* gene (Fig. 5, top section).

In the upstream region of *alkM*, an *alkR* gene (ORF5) was found in complement orientation. It encoded an AraC-XylS-like transcription regulator protein (AlkR, 310 aa). Its putative target binding site is an inverted repeat found 44 bp upstream from the −35 box (Fig. 5, top section).

Sequencing of the inverse PCR product revealed that a partial glutathione reductase (*gshR*, ORF7) gene is located downstream of *alkM* on the chromosome. This gene encodes a protein which is assumed to take part in the scavenging of reactive oxygen radicals produced in the course of *n*-alkane oxidation (Tani *et al.*, 2001). The further 5′ region of the 5445 bp long fragment consists of clustered early lipid A biosynthesis genes, such as UDP-N-acetylglucosamine acyltransferase (*lpxA*, ORF4), 3*R*-hydroxymyristoyl-acyl carrier protein dehydra-

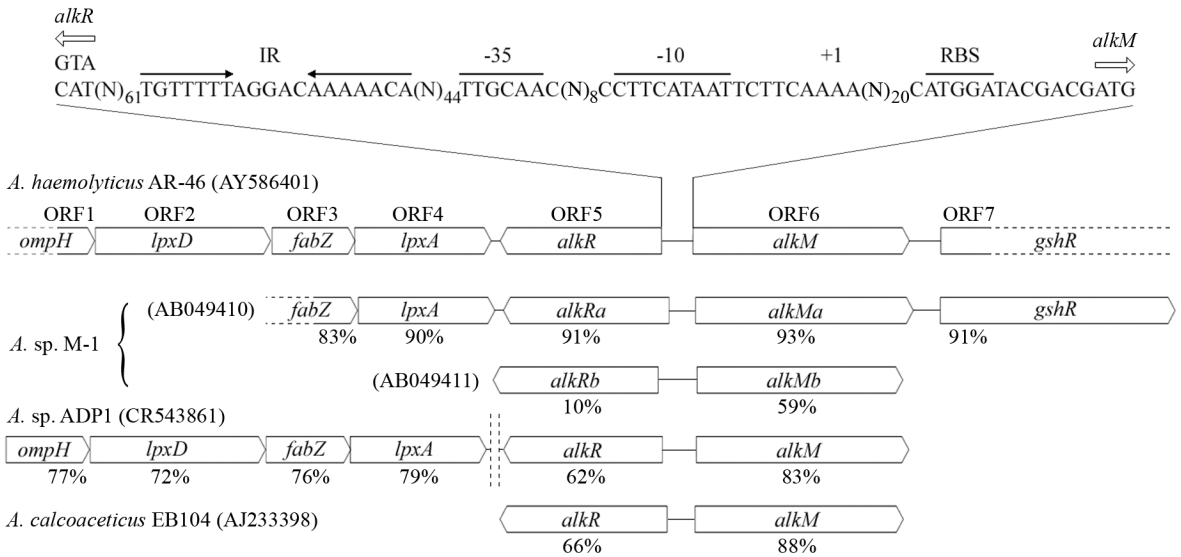


Fig. 5. (Top) The intergenic region between the *alkR* and *alkM* genes of strain AR-46 with the putative start codons (empty arrows), AlkR binding inverted repeat (IR, filled arrows), −35 and −10 promoter elements, transcription initiation site (+1) and ribosome binding site (RBS). (Bottom) Genetic arrangement of similar genes in *Acinetobacter* spp. GenBank accession numbers of cited genes are given in parenthesis. Similarity percentage values relating to corresponding genes of *A. haemolyticus* AR-46 are given below the empty arrows indicating the genes. Horizontal broken lines depict the non-sequenced part of the gene, while vertical broken lines depict the sequence gap between the indicated genes.

tase (*fabZ*, ORF3), UDP-3-*O*-3-hydroxylauroyl glucosamine *N*-acyltransferase (*lpxD*, ORF2), and a partial putative outer membrane protein (*ompH*, ORF1) gene. A systematic comparison and the arrangement of these genes in *Acinetobacter* spp. are presented in the bottom section of Fig. 5.

*A. haemolyticus* AR-46 is highly similar to *A.* sp. M-1 in genetic organization and the sequences of the encoded proteins. The early lipid A biosynthesis genes are adjacent to early *n*-alkane degradation genes. However, the *alkRb-alkMb* genes are located distinctly, and the functions of the upstream genes are not related to membrane formation in strain M-1. The *lpxD-fabZ-lpxA* genes are clustered in *A.* sp. ADP1 too, but the *alkR-alkM* genes are separated by almost 25 kbp. Besides these genes, peptidyl-prolyl *cis-trans* isomerase and acyl CoA dehydrogenase are present in strain ADP1 and in *A. calcoaceticus* EB104. Moreover, glutathione reductase is not found in complete genome-sequenced *A.* sp. ADP1 at all.

## Discussion

Strain AR-46 was isolated from the production water of an oil reservoir in Hungary. Both 16S rDNA analysis and biochemical characterization indicated the highest degree of similarity between AR-46 and the *A. haemolyticus* type strain. This is the first detailed description of an *n*-alkane-degrading isolate from the environment belonging to this species. Under aerobic conditions, AR-46 is able to assimilate *n*-alkanes with carbon chain lengths from $C_{12}$ to $C_{35}$. Among the tested compounds, *n*-hexadecane was found to be the best substrate for growth and biodegradation [$\mu_m$ = 0.253 $h^{-1}$, $Y'_{X/S}$ = 0.576 kg of cells (kg of *n*-hexadecane)$^{-1}$ at the optimal temperature of 37 °C]. A systematic comparison of AR-46 with related *Acinetobacter* spp. concerning the temperature dependence of *n*-alkane degradation was performed. Although *Acinetobacter* species are routinely maintained at 30 °C, the present results suggest a cultivation temperature of 37 °C for *A. calcoaceticus* EB104 and *A. venetianus* 6A2. The experimental data reported here indicate that this latter strain and our isolate appear to be well-suited for relevant biotechnological applications in consequence of their excellent long-chain *n*-alkane-degrading ability at both temperatures.

The high rate of *n*-alkane biodegradation must correlate with an improved substrate uptake

mechanism. Intimate interaction between the cell and *n*-alkane droplet surfaces was observed microscopically, and this adherence is involved in the solubilization and uptake process. *A. haemolyticus* AR-46 exhibits unique behaviour: its cells do not possess either the thin fimbriae (ca. 3.5 nm in diameter) observed in strain RAG-1, or the common thick (ca. 5 nm in diameter) ones correlated with twitching motility, but the diameter of the thick fimbriae (11–14 nm) of AR-46 is unusually large. These thick fimbriae of the *n*-hexadecane-adhered cells are significantly (2–3 times) longer than the fimbriae of the non-adhered and control cells (see Fig. 3), and the present study suggests that these long structures play the major role in substrate adherence and solubilization. This phenomenon is also manifested in their physiological properties. The interactions between the *n*-alkane droplets and the adhered hydrophobic cells are so strong that cells can not be separated from the substrate even by intensive centrifugation. Interestingly, however, the detached *n*-alkane-grown AR-46 cells in the bulk phase, similarly to cells grown in rich media, are predominantly unable to adhere to *n*-hexadecane because of their constant surface hydrophilicity. Fewer than 10% of these free AR-46 cells can attach to the *n*-alkane, whereas the analogous values for *A. venetianus* RAG-1 and VE-C3 are approx. 90% (Baldi *et al.*, 1999). The special dynamic balance between the hydrophobic, adhered cells with long fimbriae and the hydrophilic, detached cells with short fimbriae comprises a novel theory of alkane solubilization. The products of clustered *lpxD-fabZ-lpxA* genes located adjacently to the *alkR-alkM* gene may also play a crucial role in *n*-alkane solubilization in *A. haemolyticus* AR-46. Lipid A and associated lipopolysaccharides mainly consist of fatty acid-linked aminosugars, found in a wide range in cell components, *e. g.* extracellular emulsan, membrane-bound vesicles (Leahy *et al.*, 2003) and emulsan-like polymer on the cell surfaces (Pines *et al.*, 1983), all of which enhance the *n*-alkane bioavailability. The dynamic balance theory was strengthened by the fact that the intermediates *n*-hexadecan-1-ol and *n*-hexadecan-1-oic acid and the wax ester *n*-hexadecyl-*n*-hexadecanoate could be measured from free cells, but not from the media.

GC-MS identification of these compounds and enzyme assays afforded evidence of the involvement of the monoterminal oxidation pathway in AR-46. In support of this, the single chromosomal *alkM* gene was sequenced. Comparison of the results of Northern hybridization experiments on *A.* spp. demonstrated significant differences in alkane hydroxlase gene induction and regulation. In *A.* sp. strain M-1, the *alkMa* expression is induced only by $C_{26}-C_{30}$ *n*-alkanes, and the *alkMb* expression by $C_{16}-C_{22}$ *n*-alkanes. In contrast, induction of the *alkM* gene in AR-46 is evoked by the entire *n*-alkane range ($C_{16}-C_{30}$). The dual regulation of two *alkM* counterparts also exists in the efficient *n*-alkane degrader *A. venetianus* 6A2. Though Northern hybridization experiments were not performed, investigation of the growth-supporting substrate range of *alkM* gene disruptants indicates that *alkMa* is responsible for the degradation of the $C_{16}-C_{18}$ *n*-alkanes while *alkMb* is responsible for the $C_{10}-C_{14}$ *n*-alkanes in strain 6A2 (Throne-Holst *et al.*, 2006). Overall, the alkane induction profile depends essentially on the regulation mechanism, and not on the AlkM sequence similarity. AlkM of AR-46 displays 96% identity to AlkMa of 6A2, and 93% identity to AlkMa of M-1, but a completely different *n*-alkane pool can switch on the transcription of the *alkM* genes. The fact that strain AR-46 harbours only one *alkM* gene inducible by a wide range of *n*-alkanes can be evolutionally advantageous versus 6A2 and M-1, especially under real environmental conditions, where the hydrocarbon composition of pollution is generally diverse.

However, the presence of only one well-inducible *alkM* gene does not automatically lead to a high biodegradation rate. The *alkM* gene of *A.* sp. ADP1 is inducible by $C_{12}-C_{18}$ *n*-alkanes (not detected above; Ratajczak *et al.*, 1998b) and its protein sequence is similar to AlkM of AR-46 (83% identity). Moreover, in the upstream regions of *alkM* genes, *in silico* analysis revealed the same types of putative promoter elements and inverted repeat sequences serving binding targets for the AraC-XylS-like AlkR transcription regulator in both strains. Despite these facts, differences in AlkR sequences (62% identity), in uptake mechanisms, in subsequent oxidation processes or in other unknown features can result in great differences in degradation rates, not only between AR-46 and ADP1, but also between all *Acinetobacter* species. Otherwise, the rate of growth on *n*-hexadecane was found to be much greater for strain AR-46 than for ADP1, and this isolate is therefore a good candidate for relevant industrial applications.

Further investigations are needed to explain the unique features of the *n*-alkane metabolism of strain AR-46. Experiments are being planned to elucidate why, if *n*-hexadecane promotes the quickest growth of strain AR-46, the *alkM* gene can be induced more strongly by *n*-eicosane. As *n*-dodecane did not induce *alkM* transcription, and *n*-alkane dioxygenase and cytochrome P-450 activities were not detected in the cell extracts, the depletion of *n*-dodecane seems to occur via an unknown degradation pathway. Unfortunately, deeper genetic analyses are hampered by the very low efficiency of site-specific recombination. Similarly as for *A. haemolyticus* AR-46, deriving gene disruptants failed for strain M-1 too.

*Acknowledgements*

We thank J. B. van Beilen for providing *A.* sp. 2769A, *A. calcoaceticus* NCIB 8250, *A. calcoaceticus* 69-V and *A. calcoaceticus EB104;* P. A. Williams for providing *A.* sp. ADP-1; and M. Throne-Holst and S. B. Zotchev for providing *A. venetianus* 6A2. This work was supported by the Institute for Biotechnology, Bay Zoltán Foundation for Applied Research.

Baldi F., Ivosevic N., Minacci A., Pepi M., Fani R., Svetlicic V., and Zutic V. (1999), Adhesion of *Acinetobacter venetianus* to diesel fuel droplets studied with *in situ* electrochemical and molecular probes. Appl. Environ. Microbiol. **65**, 2041–2048.

Bradford M. M. (1976), A rapid and sensitive method for quantitation of microgram quantities of protein utilizing the principle of protein-dye binding. Anal. Biochem. **72**, 248–254.

Di Cello F., Pepi M., Baldi F., and Fani R. (1997), Molecular characterization of an *n*-alkane-degrading bacterial community and identification of a new species, *Acinetobacter venetianus.* Res. Microbiol. **148**, 237–249.

Dubois M., Gilles K., Hamilton J. K., Rebers P. A., and Smith F. (1951), A colorimetric method for the determination of sugars. Nature **168**, 167.

Engebrecht J. A., Brent R., and Kaderbhai M. A. (1991), Minipreps of plasmid DNA. In: Current Protocols in Molecular Biology (Ausubel F. M., Brent R., Kingston R. E., Moore D. D., Seidman J. G., Smith J. A., and Struhl K., eds.). John Wiley & Sons, Inc., New York, chapters 1. 6.1 and 1. 6.4.

Goldman S., Shabtai Y., Rubinovitz C., Rosenberg E., and Gutnick D. L. (1982), Emulsan in *Acinetobacter calcoaceticus* RAG-1: distribution of cell-free and cell-associated cross-reacting material. Appl. Environ. Microbiol. **44**, 165–170.

Hori K., Matsuzaki Y., Tanji Y., and Unno H. (2002), Effect of dispersing oil phase on the biodegradability of a solid alkane dissolved in non-biodegradable oil. Appl. Microbiol. Biotechnol. **59**, 574–579.

Huy N. Q., Jin S., Amada K., Haruki M., Huu N. B., Hang D. T., Ha D. T., Imanaka T., Morikawa M., and Kanaya S. (1999), Characterization of petroleum-degrading bacteria from oil-contaminated sites in Vietnam. J. Biosci. Bioeng. **88**, 100–102.

Käppeli O. and Finnerty W. R. (1979), Partition of alkane by an extracellular vesicle derived from hexadecane-grown *Acinetobacter*. J. Bacteriol. **140**, 707–712.

Koma D., Hasumi F., Yamamoto E., Ohta T., Chung S. Y., and Kubo M. (2001), Biodegradation of long-chain *n*-paraffins from waste oil of car engine by *Acinetobacter* sp. J. Biosci. Bioeng. **91**, 94–96.

Leahy J. G., Khalid Z. M., Quintero E. J., Jones-Meehan J. M., Heidelberg J. F., Batchelor P. J., and Colwell R. R. (2003), The concentrations of hexadecane and inorganic nutrients modulate the production of extracellular membrane-bound vesicles, soluble protein, and bioemulsifier by *Acinetobacter venetianus* RAG-1 and *Acinetobacter* sp. strain HO1-N. Can. J. Microbiol. **49**, 569–575.

Maeng J. H., Sakai Y., Tani Y., and Kato N. (1996), Isolation and characterization of a novel oxygenase that catalyzes the first step of *n*-alkane oxidation in *Acinetobacter* sp. M-1. J. Bacteriol. **178**, 3695–3700.

Müller R., Asperger O., and Kleber H. P. (1989), Purification of cytochrome P-450 from *n*-hexadecane-grown *Acinetobacter calcoaceticus.* Biomed. Biochim. Acta **48**, 243–254.

Pines O. and Gutnick D. (1984), Alternate hydrophobic sites on the cell surface of *Acinetobacter calcoaceticus* RAG-1. FEMS Microbiol. Lett. **22**, 307–311.

Pines O., Bayer E. A., and Gutnick D. L. (1983), Localization of emulsion-like polymers associated with the cell surface of *Acinetobacter calcoaceticus.* J. Bacteriol. **154**, 893–905.

Radwan S. S., Sorkhoh N. A., Fardoun F., and Al-Hasan R. H. (1995), Soil management enhancing hydrocarbon biodegradation in the polluted Kuwaiti desert. Appl. Microbiol. Biotechnol. **44**, 265–270.

Ratajczak A., Geissdörfer W., and Hillen W. (1998a), Alkane hydroxylase from *Acinetobacter* sp. strain ADP1 is encoded by *alkM* and belongs to a new family of bacterial integral-membrane hydrocarbon hydroxylases. Appl. Environ. Microbiol. **64**, 1175–1179.

Ratajczak A., Geissdörfer W., and Hillen W. (1998b), Expression of alkane hydroxylase from *Acinetobacter* sp. strain ADP1 is induced by a broad range of *n*-alkanes and requires the transcriptional activator AlkR. J. Bacteriol. **180**, 5822–5827.

Rosenberg E., Zuckerberg A., Rubinovitz C., and Gutnick D. L. (1979), Emulsifier of *Arthrobacter* RAG-1: isolation and emulsifying properties. Appl. Environ. Microbiol. **37**, 402–408.

Rosenberg M., Bayer E. A., Delarea J., and Rosenberg E. (1982), Role of thin fimbriae in adherence and growth of *Acinetobacter calcoaceticus* RAG-1 on hexadecane. Appl. Environ. Microbiol. **44**, 929–937.

Sakai Y., Maeng J. H., Tani Y., and Kato N. (1994), Use of long chain *n*-alkanes ($C_{13}$–$C_{44}$) by an isolate, *Acinetobacter* sp. M-1. Biosci. Biotechnol. Biochem. **58**, 2128–2130.

Sakai Y., Maeng J. H., Kubota S., Tani A., Tani Y., and Kato N. (1996), A non-conventional dissimilation pathway for long chain *n*-alkanes in *Acinetobacter* sp. M-1 that starts with a dioxygenase reaction. J. Ferm. Bioeng. **81**, 286–291.

Snellman E. A., Sullivan E. R., and Colwell R. R. (2002), Purification and properties of the extracellular lipase, LipA, of *Acinetobacter* sp. RAG-1. Eur. J. Biochem. **269**, 5771–5779.

Sullivan E. R., Snellman E. A., Baryshnikova L., and Colwell R. R. (1999), Multiple mechanisms to facilitate hydrocarbon uptake in *Acinetobacter* sp. RAG-1. Gen. Meet. Am. Soc. Microbiol. 99st, 1999. Abstr. Q-107, p. 554.

Tani A., Ishige T., Sakai Y., and Kato N. (2001), Gene structures and regulation of the alkane hydroxylase complex in *Acinetobacter* sp. strain M-1. J. Bacteriol. **183**, 1819–1823.

Throne-Holst M., Markussen S., Winnberg A., Ellingsen T. E., Kotlar H. K., and Zotchev S. B. (2006), Utilization of *n*-alkanes by a newly isolated strain of *Acinetobacter venetianus*: the role of two AlkB-type alkane hydroxylases. Appl. Microbiol. Biotechnol. **72**, 353–360.

Vaneechoutte M., Tjernberg I., Baldi F., Pepi M., Fani R., Sullivan E. R., van der Toorn J., and Dijkshoorn L. (1999), Oil-degrading *Acinetobacter* strain RAG-1 and strains described as *Acinetobacter venetianus* sp. nov. belong to the same genomic species. Res. Microbiol. **150**, 69–73.

Vold R. D. and Vold M. (1983), Colloid and Interface Chemistry. Addison-Wesley, London

Ward O., Singh A., and Van Hamme J. (2003), Accelerated biodegradation of petroleum hydrocarbon waste. J. Ind. Microbiol. Biotechnol. **30**, 260–270.

Wilson K. (1994), Minipreps of bacterial genomic DNA. In: Current Protocols in Molecular Biology (Ausubel F. M., Brent R., Kingston R. E., Moore D. D., Seidman J. G., Smith J. A., and Struhl K., eds.). John Wiley & Sons, Inc., New York, chapter 2. 4.2.